AIChE

Agglomeration Detection Based on Attractor Comparison in Horizontal Stirred Bed Reactors by Acoustic Emission Sensors

Yijia Cao, Jingdai Wang, Yijun He, Wei Liu, and Yongrong Yang
State Key Laboratory of Chemical Engineering, Zhejiang University, Hangzhou 310027, P.R. China; and
Dept. of Chemical and Biochemical Engineering, Zhejiang University, Hangzhou 310027, P.R. China

DOI 10.1002/aic.11935
Published online August 13, 2009 in Wiley InterScience (www.interscience.wiley.com).

In industrial propylene polymerization technology of Innovene and Chisso, agglomeration of polymer particles in horizontal stirred bed reactors (HSBR) has significant negative impacts on the reactor efficiency. If the hydrodynamic change could be detected early enough, then large chunks may not be formed nor cause an unscheduled shutdown of the plant. A novel non-invasive acoustic emission (AE) technique combined with an attractor comparison method is presented. It is based on the comparison of the time series of AE signals acquired from a normal state with the time series measured during operation of the bed. The nature of the method is to determine whether or not two time series are generated by the same mechanism. A statistical characteristic S *is used to test the null hypothesis that the two multidimensional probability distributions are identical. Experiments were carried out at room temperature in a 475 mm i.d. laboratory HSBR. The results demonstrated that the method is sensitive to small changes in the particle size distribution. It is, therefore, indicated that the proposed method not only can offer "early and accurate warning," but also has the potential to locate the agglomeration in HSBR with multiple AE sensors.* © 2009 American Institute of Chemical Engineers *AIChE J,* 55: 3099–3108, 2009

Keywords: agglomeration, horizontal stirred bed reactors (HSBR), polypropylene, acoustic emission (AE), attractor comparison, nonlinear analysis

Introduction

Horizontal stirred bed reactors (HSBR) used in the gas-phase polypropylene (PP) production of Innovene and Chisso have been developed in recent years.[1,2] With the development of the polypropylene industry, more and more attention has been paid to HSBR. PP manufactured by this reactor type has already taken a considerable market share, and the proportion is still growing. Novel design of axial powder mixing in HSBR is helpful to minimize the time of grade transition.[2] Condensed monomers are distributed on the powder bed of the HSBR to remove the reaction heat by their evaporation.[3] Compared to gas-phase fluidized bed reactors for polyolefins, the possibility of agglomeration in HSBR is higher because of the presence of the liquid substance. Agglomeration of polyolefin particles is one of the most important problems in multiphase reactors.[4] The formation of lumps in HSBR can lower the reactor efficiency, by plugging the discharging pipeline, breaking the heat exchange balance, and even deviating from normal flow pattern, etc. A certain degree of agglomeration might fill up most of the available reactor volume and finally lead to an unscheduled shutdown of the plant. Therefore, it is worthwhile to detect agglomeration as early as possible: taking effective measures so as to avoid the product getting into a worse condition and the unnecessary economic loss.

An ideal method for agglomeration detection must achieve two main aims. The first and more important one is "early

Correspondence concerning this article should be addressed to J. Wang at wangjd@zju.edu.cn

Figure 1. Type one: "spherical lumps" formed by hot spots in an industrial HSBR.

warning," which means detecting the trend of agglomeration before it becomes irreversible. The second is "accurate warning": it should be able to reflect the nature of the reactors although some possible environmental disturbances exist. Therefore, it will be quite important to develop an effective and robust detection method to meet "early and accurate warning."

Most current popular measurement techniques such as pressure,[5–11] temperature,[10,12] electrostatic,[13–15] and optical measurements,[16] have all been reported to detect agglomeration in fluidized bed reactors. Unfortunately, only a few articles deal with HSBR for polypropylene production, and most of them were focused on RTD,[2,17] reactor models,[1,2,18,19] and mixing mechanisms.[20,21] Only one patent[22] discussed how to minimize polymer agglomerate or lump formation in HSBR, but the fact that in the reactor agglomerations happen frequently suggests that this patent does not work well.

In recent years, acoustic measurement techniques have been developed to monitor the state of equipment and the physicochemical changes within chemical engineering processes.[23] The advantage of acoustics is that it could be considered as a non-invasive technique since direct contact with the process under investigation is not required. Recent studies have found that the AE signals mainly represent the particles information[24] while the pressure fluctuation signals mainly reflect the bubbles information[25] by comparing the multi-scale structure of AE signals with pressure fluctuation signals based on wavelet and R/S analysis. Hence, AE signals are much more reliable to monitor the random movement of particles, and their sensitivities to small changes in particle size distribution,[24,26–28] makes them possible to detect agglomeration accurately. Consequently, in this article, AE signals generated by collision between particles and the reactor wall will be used to detect agglomeration.

The analysis method we presently propose is a modification to the "attractor comparison method" developed by van Ommen et al.[9] This proposed method can detect small changes, which do not influence obviously the macro parameters (temperature, pressure, yield, etc.) of the process, but may cause unwanted impacts on the process. Moreover, we will show that this monitoring method can easily handle multiple AE signals. The experiments suggest that it is a potentially powerful monitoring tool to locate where the unwanted events are going to happen, and thus, a method for monitoring large industrial HSBR.

Characterization

The major cause of agglomeration in olefin polymerization processes is the local mismatch between the heat removal rate and the heat releasing rate. But different types of agglomeration may also be formed for different reasons. According to the shape of samples obtained from an industrial reactor, the agglomeration in HSBR fall into two types: "spherical lumps" and "flocculent sheets." The "spherical lumps" (Figure 1) are formed when local hot spots appear in the bed. The reaction heat cannot be removed because of the uneven distribution of quench liquid or improper control of the reactor temperature, and cause the heated particles to adhere to each other. "Spherical lumps" are $\sim$100 mm in diameter, containing a core composed of fused polymer and an outer surface covered with granular polymer that has fused to the core. Sometimes they are very hard and may impede product withdrawal, thereby reducing production rates, and negatively impacting product quality. On the other hand, the "flocculent sheets" are formed when the catalyst or the quench liquid is sprayed directly on the surface of the stirring paddles or the reactor wall. Incidents of "flocculent sheets" are relatively unusual, they are 20–50 mm wide and about 50 to over 100 mm long (Figure 2). However, in some extreme cases, the overall size is from a few square centimeters to several square meters (Figure 3). The "flocculent sheets" will fill in most of the available volume of the reactor and even change the flow pattern, which might lead to the unscheduled shutdown of the plant.

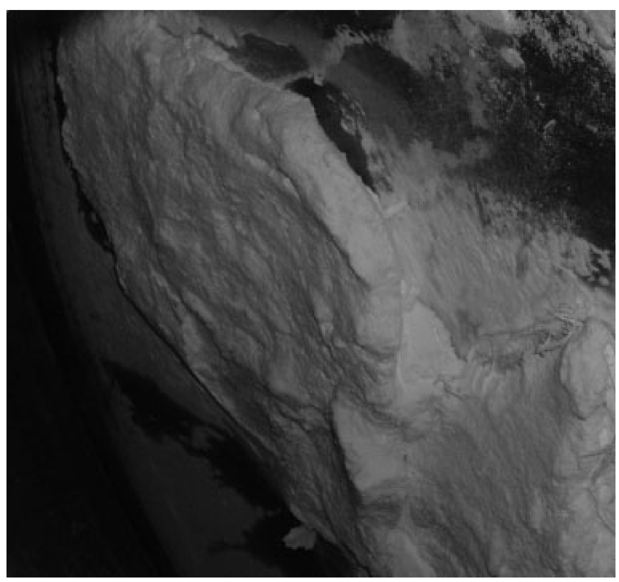

Figure 2. Type two: small "sheets" adhered to the surface of the mixing paddles in an industrial HSBR.

Figure 3. Type two: serious "flocculent sheets" occupied the head of the paddles.

Methodology

General description of the attractor comparison method

The nature of the attractor comparison method is to determine whether or not two time series are generated by the same mechanism. Diks et al.[29] proposed a statistical characteristic S for testing the null hypothesis that two multidimensional probability distributions are identical. The statistical characteristic S is defined as the ratio of $\hat{Q}$ to the square root of $V_c(\hat{Q})$ shown in Eq. 1,

$$S = \frac{\hat{Q}}{\sqrt{V_c(\hat{Q})}} \tag{1}$$

where $\hat{Q}$ is an unbiased estimator of the square of a distance between the two probability distributions and $V_c(\hat{Q})$ is the variance of the estimator $\hat{Q}$, and it is a random variable with zero mean and standard deviation equal to 1 under the null hypothesis. Moreover, as Diks et al.[29] pointed out, the null hypothesis can be rejected when the estimated values of S are larger than 3, which is supported by the fact that the probability of finding the value of S larger than 3 is smaller than 0.05.[29]

On the basis of the approach discussed earlier, van Ommen et al.[9] proposed a method based on reconstruction of an attractor from a pressure fluctuation signal for early detection of changes in fluidization behavior. For the application of the attractor comparison method to AE signals, we follow the same approach as proposed by van Ommen et al.[9] The current method is also based on a comparison of a reference time series of AE signals, reflecting a certain required or accepted state of the HSBR dynamics, with successive time-series measured during operation of the bed. Since van Ommen et al.[9] transformed the time series x_k into a set $X_i = (x_{(i-1)m+1}, x_{(i-1)m+2}, \ldots, x_{i\cdot m})^T$ this makes the total calculation procedure a factor m^2 times faster, which is much more useful for AE signals sampled in higher frequency than pressure fluctuation.

Implementation details

Sampling Frequency. The basic principle of determining sampling frequency is to choose a relatively low sampling frequency while ensuring that no information contained in the signals is lost. According to the Nyquist theorem, the sampling rate should be fast enough (more than two times) to record all frequencies. Figures 4a, b show the power spectral density of AE signals of HSBR with and without PP4, respectively. The resulting power spectral density show prominent frequencies at ~2500 Hz and 4000 Hz. All the signal energy is concentrated below 8000 Hz, meaning that the sampling frequency of 20 kHz is high enough to record all information from the signals. The frequency components

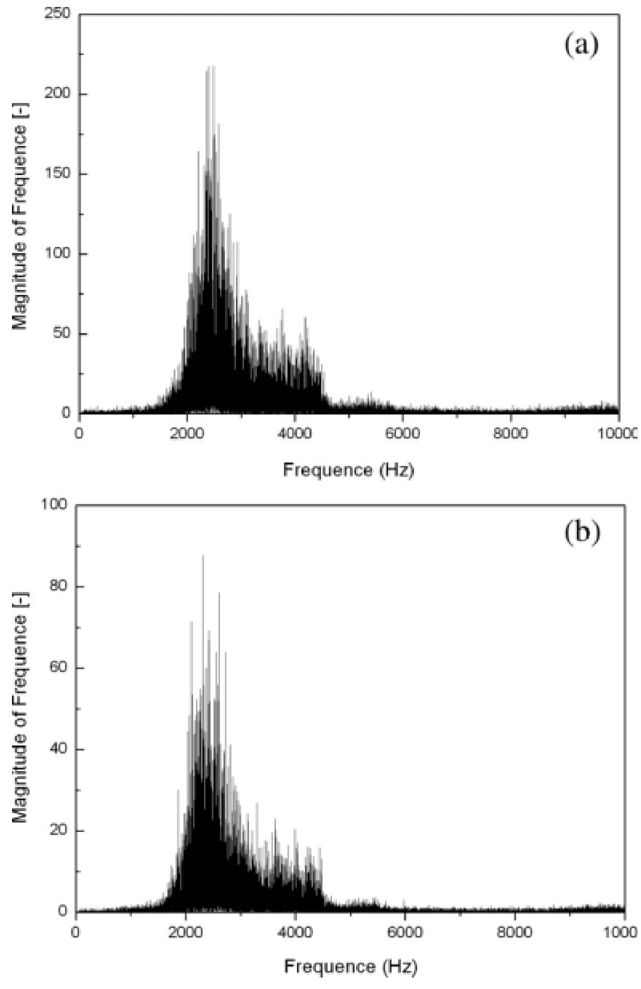

Figure 4. (a) Power spectral density of AE signals sampled under "reference" condition (agitator speed: 20 rpm, bed mass: 40 kg, Fs: 20,000 Hz) for PP1. (b) Power spectral density of AE signals sampled under "evaluation" condition (agitator speed: 20 rpm, bed mass: 40 kg, Fs: 20,000 Hz) for PP1 mixed with PP4 (mass fraction: 0.1).

of both figures are similar. The phases are so similar that a reliable method could not be developed to detect agglomeration by examining specific frequency bands, such as the 2500 Hz region.

Preprocessing. As a standard procedure, we normalize the data by subtracting the mean and dividing by the standard deviation,[30] as shown in Eq. 2.

$$x_k = \frac{A_k - \bar{A}}{\sigma_A} \tag{2}$$

Since the presence of noise in a time-varying signal restricts one's ability to obtain meaningful information from the signal, a noise-reduction algorithm[31] based on the wavelet transform is used to purify the AE signals. The threshold of the noise-reduction algorithm is determined automatically by the process,[31] which makes noise-reduction of AE signals more convenient. The experimental results show that it is really able to reduce the noise mixed in the AE signals, especially that generated by the agitator and motor.

Experimental

Four types of experiments were carried out to optimize the attractor comparison parameters, and test the influences of agitator speed, compressed air flow rate, and particle size distribution on the new monitoring method.

1) Experiments with stepwise changes in the agitator speed.

2) Experiments with stepwise changes in the compressed air flow rate.

3) Experiments with stepwise changes in the particle size distribution.

4) Experiments with gradual changes in the particle size distribution.

Experimental facilities and operation conditions

Four kinds of polypropylene were used in the cold mold experiments with physical properties shown in Table 1. The particle size distributions were determined by a laser diffraction system (Malvern Mastersizer 2000).

All the experiments were carried out in a cold mold of laboratory scale which is made of Plexiglas, 475 mm i.d. with a 1530 mm long and the four paddles agitator (Figure 5). The compressed air from a blower was blown into the reactor from the bottom* through four lines with individual flowmeters (0–10 m^3/h). The agitator speed (0–75 rpm) was controlled by an inverter (FangH F66-B IGBT, China), and the variation of the torque was recorded by a computer. All the experiments were carried out at room temperature.

AE measurement and data acquisition

The acoustic emission signals online collection and analysis system was developed by the UNILAB Research Center of Chemical Engineering in Zhejiang University, China. It consists of AE sensors, a preamplifier, a signal conditioning system, and a data acquisition system. The transducer used in this study is a piezoelectric resonant accelerometer, which is used to collect the acceleration of vibration without the noise transferred via the air (PXR02, 20 kHz, 10–70 kHz, 70 dB, China)†. The transducer is attached non-invasively to the outside of the vessel at a position of 1/4 D above the bottom (as shown in Figure 6) with a sampling frequency of 20 kHz. An acoustic coupling agent is used to transfer the acoustic emission in the vessel to the transducer. For temporary installations, silicone grease is used to hold the transducer in place. For permanent installations, an adhesive holds the transducer in place and acts as an effective acoustic-coupling agent. The preamplifier (PXPA III, 5–200 kHz, China) supplies sufficient gain for the signal to be "driven" down a cable, which can be up to 200 m in length. The signal conditioning system used in the experiments is PXMA signal conditioning equipment (PXMA, China). It provides additional gain and filters the signals with a low-pass cutoff frequency of 50 kHz. The data acquisition system consists of a data acquisition card (NI PCI-6071E, National Instruments) and a personal computer. The AE signals generated by the piezoelectric accelerometer are amplified, and conditioned. Finally, they are transferred to the data acquisition card connected to the computer, controlled by the software package Labview.

Table 1. Particle Properties of the Polypropylene used in the Experiments

Particle Type	d_{10} (μm)	d_{50} (μm)	d_{90} (μm)	$D_{\text{vol. weighted mean}}$ (μm)
PP1	342.8	572.3	924.2	606.2
PP2	427.9	677.1	1061.2	714.8
PP3	404.8	703.1	1183.3	753.7
PP4	524.0	939.3	1502.0	974.8

Results and Discussion

Parameter settings

To power the monitoring method, four parameters in the attractor comparison method should be carefully adjusted. An optimization method is then adopted to find the right parameters, which should lead to an S value close to 0, when two AE time series are measured under similar hydrodynamic conditions, and a maximally high S value under different conditions. A part of the data from the experiments with stepwise changes in the particle size distribution (Type 3 classified in the experimental section) is used to optimize the parameters. By definition, the S values will increase with the increasing discrepancy between reference and evaluation time series. On the other hand, adding more PP4 into the reactor will increase this discrepancy. Hence, that the S values increase with increasing fraction of PP4 should be considered as constraints in the parameter optimization process. The optimal parameter values are given in Table 2, and these values are not the direct result of the optimization method but a minor deviation from it since limited changes only have a minor influence on the test results.[9]

*Here "bottom" does not mean right below the agitator shaft, but 5° left from the cross section view (Figure 6).

†Parameters of the sensor used in the experiments, resonance frequency: 20 kHz, band width at 10 dB: 10–70 kHz, sensitivity: 70 dB.

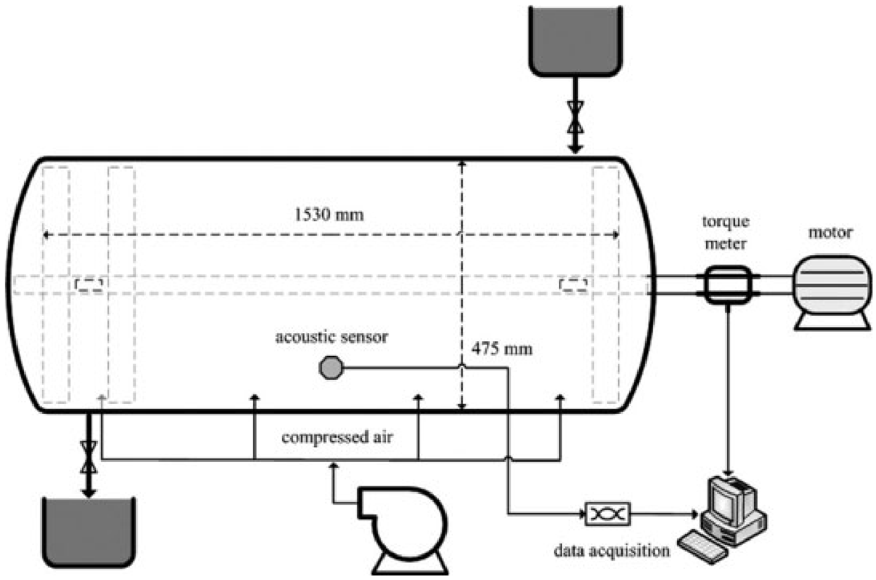

Figure 5. Schematic diagram of experimental apparatus.

Figure 7 shows the effect of these four parameters on the outcome of the test: time window (a), embedding dimension (b), bandwidth (c), and segment length (d). The AE time series were measured at 1/4 D above the bottom, stirred at 20 rpm with bed mass 40 kg, and compressed air flow rate 16 m^3/h (4 × 4 m^3/h). The reference time series were measured in a bed of pure PP1, while another two time series measured was used as the evaluation time series: one was measured at the same conditions as the normal situation and the other was measured for a different bed composition (10 wt % of PP4) as the "agglomeration" situation. All time series have a length of 50 s.

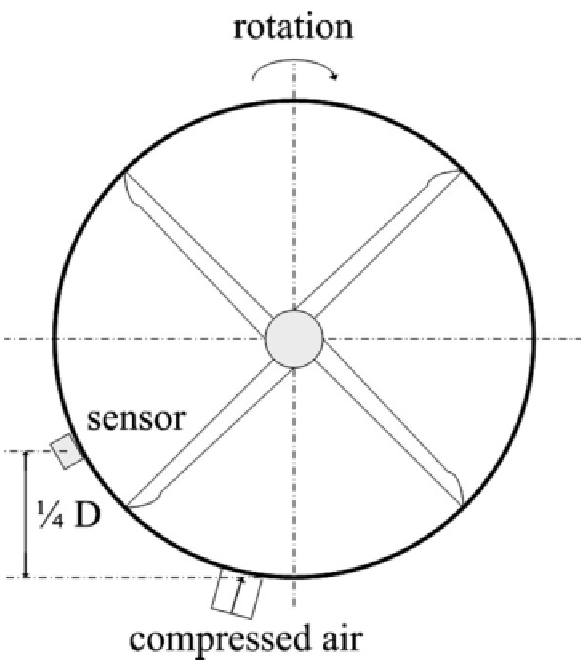

Figure 6. Cross section diagram of the experimental apparatus.

The selection criteria of the four parameters and their meaning have already been discussed in detail by van Ommen et al.,[9] therefore, repetitive discussions will be omitted. Besides, we would like to point out the choice of the bandwidth d, which sets the length scale of the smoothing. Since d will be increased by the increase of embedding dimension m, which means that the variation of d is enlarged, it may bring difficulties in practice. To constrain the parameter d in a range of 0 to 1 for convenience, a normalization procedure is used. The function $h(Z_i, Z_j)$ introduced by van Ommen et al.[9] to calculate the estimator $\hat{Q}$ is shown in Eq. 3.

$$h(Z_i, Z_j) = e^{-|Z_i - Z_j|^2/(4d^2)} \tag{3}$$

We define a new matrix D_{ij} as

$$D_{ij} = |Z_i - Z_j| \tag{4}$$

then we can normalize D_{ij} to $\tilde{D}_{ij}$ by

$$\tilde{D}_{ij} = \frac{D_{ij} - \min(D_{ij})}{\max(D_{ij}) - \min(D_{ij})} \tag{5}$$

Diks et al.[29] argued that the choice of bandwidth d was not that of optimally estimating densities but rather that of finding the proper one for which the test was most powerful. Figure 7c shows that (1) the optimal bandwidth lies between 0.45 and 0.6, and (2) a bandwidth d of 0.52 yields good test results.

Sensitivity to changes in agitator speed

The variation of the agitator speed may influence the average time cycle of the particles, and hence lead to the change of the optimal settings for the time window and embedding dimension. We have not found a good method to entirely reduce the sensitivity to the agitator speed. However, the

Table 2. **Optimal Parameter Settings for Applying the Attractor Comparison Test to the HSBR AE Signals**

Time Window	Segment Length (L)	Embedding Dimension (m)	Band Width (d)
0.2 s	4 s	2000	0.52

alternative algorithm[31] for noise reduction using a discrete wavelet transform is helpful in case of limited deviations around the operation parameter. Figure 8 shows that the agitator speed influences considerably on the experimental results. For variations of the agitator speed smaller than 10%, the S values after denoising stay below 3. For larger variations, the denoising method cannot remove the influence of the agitator speed on S, so the entire method is no more applicable.

To stabilize continuous operation, the industrial agitator speed is set to a constant. Even during grade transition, the speed will vary no more than 5%. This characteristic makes our method applicable to industrial equipment with the help of the denoising method.

Sensitivity to changes in compressed air flow rate

Compared to agitator speed in industrial HSBR, the variation of gas flow rate is much greater. In some cases, it could even reach 50%. Careful experimental observation showed that the air flow rate around the inlets not only changes the voidage of polymer bed, but also the collision between particles and internal wall of the reactor, and thus, the AE signals. However, the design of the reactor required that the particles in HSBR are in a subfluidized regime.[3] In other words, the affected areas are constrained generally underneath the polymer bed around the inlets. By carefully choosing the positions of the acoustic sensor, the effects of air flow rate could be minimized.

Figure 9 compares the S values from the signals at different positions. For a sensor located between 1/2 D and 1/8 D, the S values stay below 3. For location of 1/4 D, the S values are the least sensitive to the air flow rate, whereas at

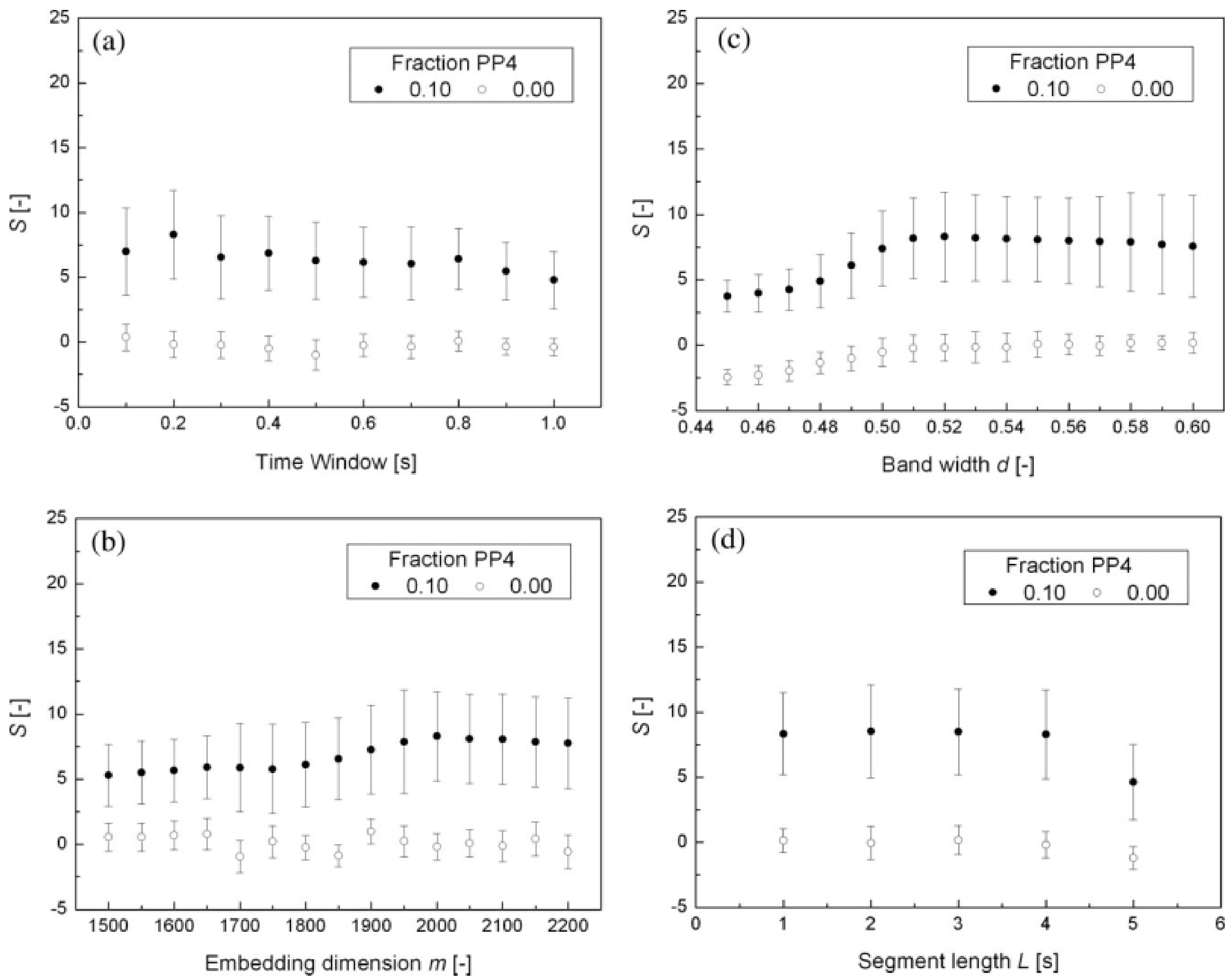

Figure 7. Influence of time window (a), embedding dimension *m* (b), bandwidth *d* (c), and segment length *L* (d) on the results of the attractor comparison test.

The points give the average of 10 or 9 S values, for 0 wt % and 10 wt % PP4, respectively. The error bars indicate the standard deviation. The reference time series has been measured in a bed with 0 wt % PP4.

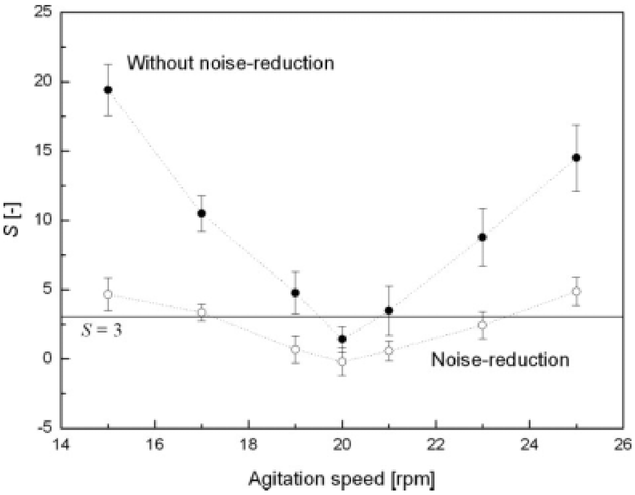

Figure 8. Influence of the agitator speed on the S value. The reference time series has been measured at 20 rpm.

At each agitator speed, 10 time series have been evaluated with and without noise-reduction. The points give the average of 10 S values, and the error bars indicate the standard deviation. The solid line at $S = 3$ indicates the statistical limit above which a significant change has taken place.

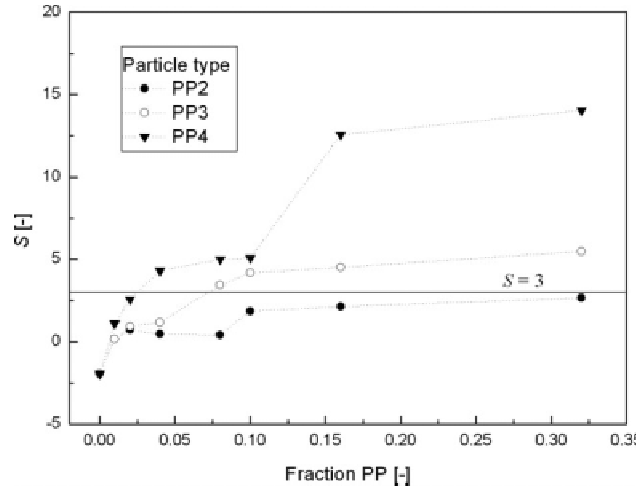

Figure 10. Detection of changes in the particle-size distribution.

The reference time series have been measured in a bed containing only PP1. The evaluated time series have been measured at eight fractions with three kinds of particles. The AE signals have been measured at 1/4 D above the bottom, with a bed mass of 40 kg, agitator speed of 20 rpm, and compressed air flow rate 4 m^3/h (each line). At each fraction, five time series have been evaluated. The points give the average of five S values, and the solid line at $S = 3$ indicates the statistical limit above which a significant change has taken place.

1/16 D, the most sensitive, because 1/16 D is located closest to and most influenced by the air inlets. The sensor at 1/2 D is near the surface of the bed and is easily disturbed by the agitator speed. Hence, we should select an appropriate detection position of sensors to reduce the various external disturbances. According to our experiments, the allowable position for AE sensors monitoring HSBR should be between 1/8 D and 1/2 D; the optimal position is 1/4 D.

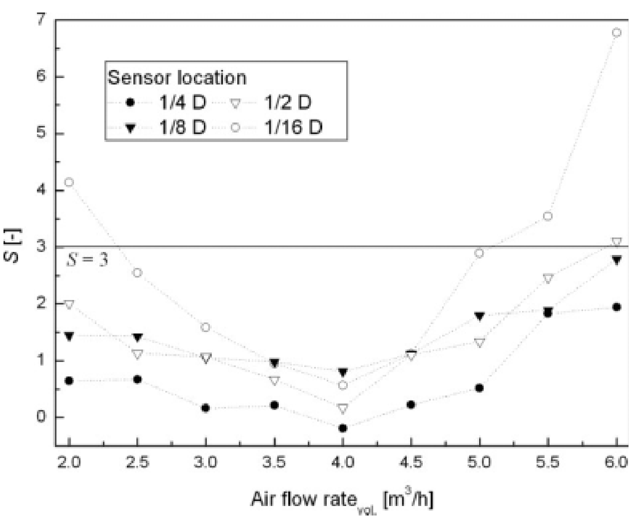

Figure 9. Influence of the air flow rate on the S value.

The time series have been measured with the acoustic sensor located at 1/2 D, 1/4 D, 1/8 D, and 1/16 D. The reference time series has been measured at 4.0 m^3/h. At each flow rate, five time series have been evaluated. The points give the average of five S values, and the solid line at $S = 3$ indicates the statistical limit above which a significant change has taken place.

Detection of changes in particle size distribution

The first experiment was carried out to illustrate the influence of a change in the particle size distribution on the S values. Three kinds of polypropylene particles (PP2, PP3, and PP4) with different sizes shown in Table 1 were added to get a stepwise change in the particle size distribution of the bed (pure PP1 at first). The reference time series with a length of 250 s has been measured in a pure PP1 bed and three sets of evaluated time series with the same length have been measured in a bed mixed with PP2, PP3, and PP4. The other conditions for all the time series were the same.

It can be seen from Figure 10 that (1) the S values will increase with the increasing PP fraction, (2) when adding the biggest particles (PP4) into the reactor, S already detects a significant change in the hydrodynamics at a PP4 fraction of 0.04, while with the smallest particles (PP2), S will not get across the solid line $S = 3$ until the fraction of PP2 exceeds 0.32. It means that the proposed method is sensitive to the small changes in particle size distribution with the formation of relatively large particles, but insensitive to the formation of medium-size or small-size particles. This characteristic is considered to have positive and negative aspects when the method is applied in industrial HSBR to detect agglomeration. The advantage is that it can effectively detect and offer "early warning" on the situations of particles growing up rapidly, for example, appearance of a hot spot resulting from high local concentration of catalyst, which can be called "fast agglomeration." On the other hand, it can be inferred from the sensitivity to "medium-size" or "small-size particle" that the "slow agglomeration" cannot be detected until the agglomerates are sufficiently large. This is a disadvantage for industrial practice. However, most of the "slow

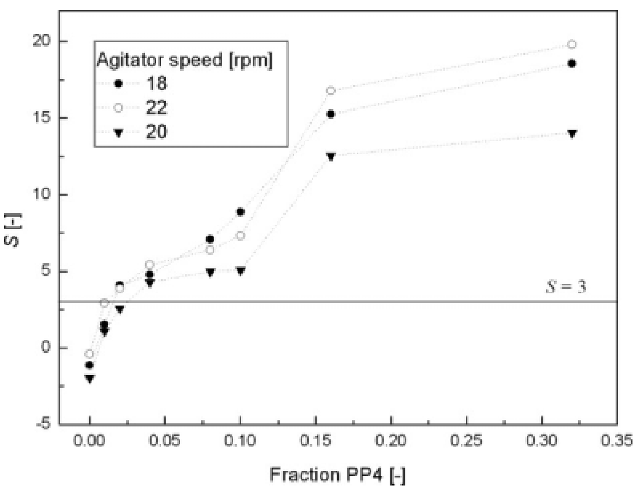

Figure 11. Influence of the agitator speed on the *S* value.

The reference time series have been measured in a bed containing only PP1. The evaluated time series have been measured at eight fractions and three agitator speeds. The AE signals have been measured at 1/4 *D* above the bottom, with a bed mass of 40 kg and compressed air flow rate 4 m^3/h (4 m^3/h each line, 16 m^3/h in all). At each fraction, five time series have been evaluated. The points give the average of five *S* values, and the solid line at $S = 3$ indicates the statistical limit above which a significant change has taken place.

agglomeration'' is formed because of small drifts of some key parameters from their set points. Fortunately, these circumstances could be tackled by resorting to advanced supervisory control system, and the chance of ''slow agglomeration'' can be minimized correspondingly.

The next two experiments tested the influences of agitator speed and air flow rate on the *S* values with changes in the particle size distribution. Figure 11 shows that the *S* values not only depend on the fraction of PP4 but also on the agitator speed, especially at a sufficiently high volume fraction. Generally, the *S* values at higher or lower agitator speed are larger than the middle speed, because the different agitator speeds lead to different types of collision between the particles and the internal wall of the reactor. Fortunately, the denoising method mentioned earlier is working and the critical points for *S* values larger than 3 are detected correctly.

The results in Figure 12 are satisfactory. For any PP4 fraction, the *S* values remain almost constant for different air flow rates. It is exciting that an optimal position for AE sensors can decrease the influence of air flow rate.

Detection of grade transition by a multiple-signal method

Present market needs combined with the broad range of polyolefin applications have forced the polyolefin industry to operate under frequent grade transition policies.[32,33] During a transition from one grade to another, the dynamic behavior might be changed in a nonlinear way due to the complex polymerization kinetics and energy effects. What will happen to the *S* values? Can the monitoring method indicate if a new stationary situation has been reached after an imposed change[9] in HSBR? To illustrate the evolution of *S* values during a grade transition, we carried out an experiment of 100 min duration with a ''grade transition'' from PP1 to PP3 (Type 4).

The cold-flow model with a continuous feed and removal of solids in which the particle size distribution of the bed is changing was used to simulate the process of grade transition. The reference time series was measured in a bed initially filled with pure PP1. Four AE sensors distributed uniformly on the outside of the vessel at the same height (1/4 *D*) recorded the signals from four different zones of the reactor. Three minutes after starting, PP3 was introduced into the reactor. The feeding rate of PP3 was 1.35 kg/min, and the discharging rate was the same to keep a constant bed mass. Consequently, more and more PP3 mixed with PP1 by stirring changed the composition of the bed over time. One minute long AE time series were evaluated using the comparison method; the AE time series measured during the first 3 min of the experiment served as the reference time series (four sensors had four reference time series individually).

Figure 13 shows the evolution of the *S* values in four different zones. The shapes of the *S* curves are approximately the same. They are rising gradually, then approach equilibrium, and finally stay at around 6. This indicates two points: first, the hydrodynamic behaviors have changed from one state to another since *S* values exceed the solid line; and second a new stationary situation has been reached.

Figure 13 also shows that (1) the main difference among the four curves is the time when *S* attains its maximum, and (2) the time lag between the two successive zones gets longer. These findings imply that PP3 in the bed is flowing from zone 1 to zone 4 roughly in a plug-flow pattern with

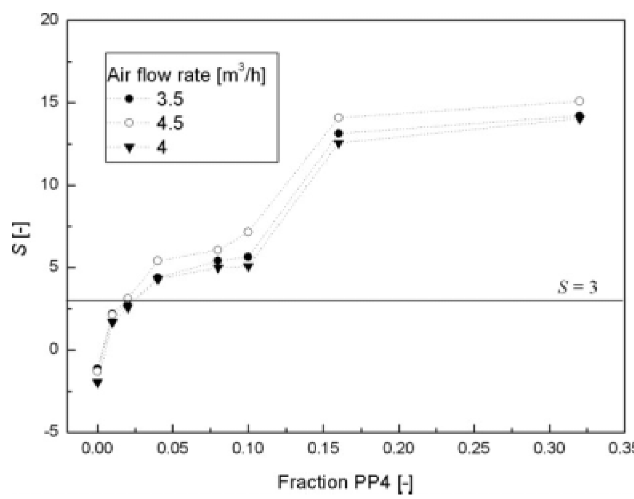

Figure 12. Influence of the air flow rate on the *S* value.

The reference time series have been measured in a bed containing only PP1. The evaluated time series have been measured at eight fractions and three air flow rates. The AE signals have been measured at 1/4 *D* above the bottom, with a bed mass of 40 kg and agitator speed 20 rpm. At each fraction, five time series have been evaluated. The points give the average of five *S* values, and the solid line at $S = 3$ indicates the statistical limit above which a significant change has taken place.

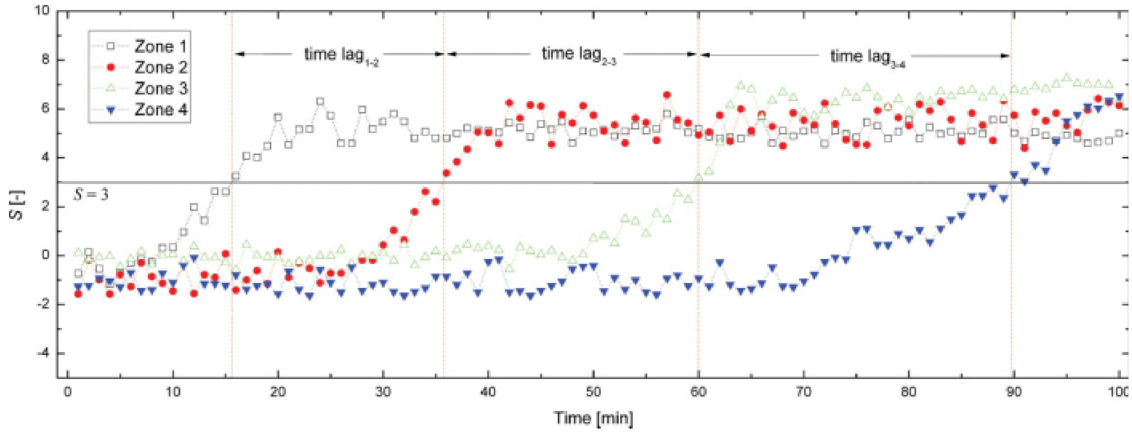

Figure 13. Evolution of *S* values for the grade change experiments.

The *S* values have been calculated for a grade transition from PP1 to PP3. The reference time series have been measured in a bed containing only PP1. Four AE sensors located at the same height (1/4 *D*) were used to measure the signals from the four zones of the reactor. The mass flow rate of PP3 added into the reactor was 1.35 kg/min, and the discharging rate was kept at the same level to maintain the bed mass. The solid line at $S = 3$ indicates the statistical limit above which a significant change has taken place. [Color figure can be viewed in the online issue, which is available at www.interscience.wiley.com.]

the presence of backmixing. The results coincide with the literature reports.[2,17]

A simple four cells in a series model seems to be able to explain the experimental results, but it is not our focus in this article. However, a new function of the monitoring method has foreseen from the results of multiple-sensor experiments: localization of agglomeration. Since the AE sensors are able to collect the signals without mutual interference, agglomeration or zones where abnormality occurs in a large HSBR can be located by multiple AE sensors. A more extensive investigation of this aspect is needed to be carried out in the near future.

Conclusions

A novel non-invasive method based on acoustic emission (AE) has been presented for early detection of agglomeration in horizontal stirred bed reactors (HSBR). Since the AE signal is sensitive to small changes in the particle size distribution, it means that AE techniques are able to detect agglomeration in an environmental friendly way with fairly good accuracy.

The attractor comparison method is based on a general distance concept between multidimensional distributions. By comparing the attractor of a reference AE time series at the normal operating conditions with the attractor of evaluated AE time series acquired during operation of HSBR, we are able to get the "distance" (which is called *S* value in a statistical way) between the two distributions. An *S* value close to zero, under the null hypothesis, indicates a similar evaluated situation to the normal operating condition; while an *S* value larger than 3 indicates that the hydrodynamic behaviors in the evaluated situation have changed and agglomeration might have formed.

External factors affecting the performance of the method have been reduced. A denoising algorithm based on a discrete wavelet transform has been used to remove a part of the noise from the agitator which makes the method insensitive to small changes in the agitator speed. Carefully choosing of the AE sensors positions decreases the sensitivity of the *S* values to the air flow rate in a lab-scale research. The allowable range for AE sensors is 1/8 *D* to 1/2 *D* above the bottom; and the optimal position is 1/4 *D*.

The AE technique based on the attractor comparison method is sensitive to small changes in the particle size distribution, which means it possible to offer "early and accurate warning" of agglomeration in HSBR. Furthermore, the monitoring method can not only indicate the reach of new stationary situation during a grade transition, but also locate the agglomeration in HSBR with multiple-sensors. However, further experimental research is needed before applying the method in an industrial HSBR for agglomeration detection.

Acknowledgments

The authors thank the two anonymous reviewers who provided useful comments on the manuscript. The following students in Zhejiang University are acknowledged: Huang Zhengliang, Jiang Xiaojing, Qin Wei, and Wang Bin. The experimental data presented here could not have been accomplished without their help. They also acknowledge the financial support and encouragement of the National Natural Science Foundation of China (through No. 20676114, 20736011 and 20490205) and National High Technology Research and Development Program of China (2007AA030208).

Notation

A_k = vector of AE values
$\bar{A}$ = average of AE values, V
d = band width for smoothing of points in the state space
D = interior diameter, m
D_{ij} = matrix of $|Z_i - Z_j|$
$\hat{D}_{ij}$ = normalized matrix of $|Z_i - Z_j|$
F_s = sampling frequency, Hz
$h(Z_i, Z_j)$ = function defined in Eq. 4
L = segment length
m = embedding dimension
$\hat{Q}$ = estimator for Q
R_f = reducing factor
S = estimator for the normalized squared distance between two attractors
T_w = time window, s
$V_c(\hat{Q})$ = conditional variance of $\hat{Q}$

x_k = normalized AE values in reference time series
X_i = vector of normalized AE values in reference time series
σ_A = standard deviation of AE values, V

Literature Cited

1. Gorbach AB, Naik SD, Ray WH. Dynamics and stability analysis of solid catalyzed gas-phase polymerization of olefins in continuous stirred bed reactors. *Chem Eng Sci*. 2000;55:4461–4479.
2. Dittrich CJ, Mutsers SMP. On the residence time distribution in reactors with non-uniform velocity profiles: the horizontal stirred bed reactor for polypropylene production. *Chem Eng Sci*. 2007;62: 5777–5793.
3. Jezl JL, Peters EF, Winfield. *Horizontal Reactor for the Vapor Phase Polymerization of Monomers*. U.S. Patent 4101289, Application No. 760639. July 18, 1978.
4. van den Bleek CA, Coppens MO, Schouten JC. Application of chaos analysis to multiphase reactors. *Chem Eng Sci*. 2002;57: 4763–4778.
5. Schouten JC, van den Bleek CM. Monitoring the quality of fluidization using the short-term predictability of pressure fluctuations. *AIChE J*. 1998;44:48–60.
6. van Ommen JR, Schouten JC, Coppens MO, van den Bleek CM. Monitoring fluidization by dynamic pressure analysis. *Chem Eng Technol*. 1999;22:773–775.
7. van Ommen JR, Schouten JC, van den Bleek CM. Monitoring fluidization dynamics for detection of changes in fluidized bed composition and operating conditions. *J Fluids Eng Trans ASME*. 1999; 121:887–894.
8. van Ommen JR, Schouten JC, vander Stappen MLM, van den Bleek CM. Response characteristics of probe-transducer systems for pressure measurements in gas-solid fluidized beds: how to prevent pitfalls in dynamic pressure measurements. *Powder Technol*. 1999;106: 199–218.
9. van Ommen JR, Coppens MO, van den Bleek CM, Schouten JC. Early warning of agglomeration in fluidized beds by attractor comparison. *AIChE J*. 2000;46:2183–2197.
10. Scala F, Chirone R. Characterization and early detection of bed agglomeration during the fluidized bed combustion of olive husk. *Energy Fuels*. 2006;20:120–132.
11. Nijenhuis J, Korbee R, Lensselink J, Kiel JHA, van Ommen JR. A method for agglomeration detection and control in full-scale biomass fired fluidized beds. *Chem Eng Sci*. 2007;62:644–654.
12. Hulet C, Llinas JR, Selo JL, Briens C, Thomas S, Mouillet A. Multivariate analysis of process signals for early detection of agglomeration in a gas phase fluidized bed for polyethylene. *Chem Eng Process*. 2008;47:1224–1233.
13. Gajewski A. Investigation of the electrification of polypropylene particles during the fluidization process. *J Electrostat*. 1985; 17: 289–298.
14. Briens CL, Briens LA, Barthel E, Le Blevec JM, Tedoldi A, Margaritis A. Detection of local fluidization characteristics using the V statistic. *Powder Technol*. 1999;102:95–103.
15. Hendrickson G. Electrostatics and gas phase fluidized bed polymerization reactor wall sheeting. *Chem Eng Sci*. 2006;61:1041–1064.
16. Yu ZQ, Chow PS, Tan RBH. Quantification of particle morphology by boundary Fourier transform and generic Fourier transform. *Chem Eng Sci*. 2007;62:3777–3786.
17. Zacca JJ, Debling JA, Ray WH. Reactor residence-time distribution effects on the multistage polymerization of olefins. II. Polymer properties: bimodal polypropylene and linear low-density polyethylene. *Chem Eng Sci*. 1997;52:1941–1967.
18. Khare NP, Lucas B, Seavey KC, Liu YA, Sirohi A, Ramanathan S, Lingard S, Song YH, Chen CC. Steady-state and dynamic modeling of gas-phase polypropylene processes using stirred-bed reactors. *Ind Eng Chem Res*. 2004;43:884–900.
19. Caracotsios M. Theoretical modeling of Amoco's gas phase horizontal stirred bed reactor for the manufacturing of polypropylene resins. *Chem Eng Sci*. 1992;47:2591–2596.
20. Laurent BFC, Bridgewater J, Parker DJ. Motion in a particle bed agitated by a single blade. *AIChE J*. 2000;46:1723–1734.
21. Laurent BFC, Bridgwater J. Performance of single and six-bladed powder mixers. *Chem Eng Sci*. 2002;57:1695–1709.
22. Lin CH, Stevens JF, Tovrog BS, Rose PM. *Method and Apparatus for Minimizing Polymer Agglomerate or Lump Formation in a Gas-Phase Polypropylene Polymerization Reactor*. U.S. Patent 4921919, Application No. 202092. May 1, 1990.
23. Boyd JWR, Varley J. The uses of passive measurement of acoustic emissions from chemical engineering processes. *Chem Eng Sci*. 2001;56:1749–1767.
24. Jiang XJ, Wang JD, Jiang BB, Yang YR, Hou LX. Study of the power spectrum of acoustic emission (AE) by accelerometers in fluidized beds. *Ind Eng Chem Res*. 2007;46:6904–6909.
25. Zhao GB, Yang YR. Multiscale resolution of fluidized-bed pressure fluctuations. *AIChE J*. 2003;49:869–882.
26. Halstensen M, Esbensen K. New developments in acoustic chemometric prediction of particle size distribution—the problem is the solution. *J Chemometr*. 2000;14:463–481.
27. Leach MF, Rubin GA, Williams JC. Particle size distribution characterization from acoustic emissions. *Powder Technol*. 1978;19: 157–167.
28. Tsujimoto H, Yokoyama T, Huang CC, Sekiguchi I. Monitoring particle fluidization in a fluidized bed granulator with an acoustic emission sensor. *Powder Technol*. 2000;113:88–96.
29. Diks C, van Zwet WR, Takens F, DeGoede J. Detecting differences between delay vector distributions. *Phys Rev E Stat Nonlin Soft Matter Phys*. 1996;53:2169–2176.
30. Bai D, Bi HT, Grace JR. Chaotic behavior of fluidized beds based on pressure and voidage fluctuations. *AIChE J*. 1997;43:1357–1361.
31. Roy M, Kumar VR, Kulkarni BD, Sanderson J, Rhodes M, vander Stappen M. Denoising algorithm using wavelet transform. *AIChE J*. 1999;45:2461–2466.
32. Kadam JV, Marquardt W, Srinivasan B, Bonvin D. Optimal grade transition in industrial polymerization processes via NCO tracking. *AIChE J*. 2007;53:627–639.
33. Padhiyar N, Bhartiya S, Gudi RD. Optimal grade transition in polymerization reactors: a comparative case study. *Ind Eng Chem Res*. 2006;45:3583–3592.

Manuscript received Aug. 2, 2008, and revision received Apr. 1, 2009.